

ORIGINAL ARTICLE

Salermide, a Sirtuin inhibitor with a strong cancer-specific proapoptotic effect

E Lara¹, A Mai², V Calvanese¹, L Altucci³, P Lopez-Nieva¹, ML Martinez-Chantar⁴, M Varela-Rey⁴, D Rotili², A Nebbioso³, S Ropero¹, G Montoya⁵, J Oyarzabal⁶, S Velasco⁷, M Serrano⁷, M Witt⁸, A Villar-Garea⁹, A Inhof⁹, JM Mato⁴, M Esteller¹⁰ and MF Fraga^{1,11}

¹Cancer Epigenetics Laboratory, Spanish National Cancer Research Centre (CNIO), Madrid, Spain; ²Dipartimento di Studi Farmaceutici, Istituto Pasteur, Fondazione Cenci Bolognetti, Università degli Studi di Roma 'La Sapienza', Roma, Italy; ³Dipartimento di Patologia Generale, Seconda Università degli Studi di Napoli, Napoli, Italy; ⁴CIC bioGUNE, CIBERehd, Bizkaia Technology Park, Bizkaia, Spain; ⁵Macromolecular Crystallography Group, Spanish National Cancer Research Centre (CNIO), Madrid, Spain; ⁶Computational Chemistry Group, Spanish National Cancer Research Centre (CNIO), Madrid, Spain; ⁷Tumour Suppression Group, Spanish National Cancer Research Centre (CNIO), Madrid, Spain; ⁸Bruker Daltonik GmbH, Bremen, Germany; ⁹Histone Modifications Group, Adolf-Butenandt Institut, University of Munich, Munich, Germany; ¹⁰Cancer Epigenetics and Biology Program (PEBC), Catalan Institute of Oncology (ICO), Barcelona, Spain and ¹¹Department of Immunology and Oncology, Centro Nacional de Biotecnología/CSIC, Cantoblanco, Madrid, Spain

Sirtuin 1 (Sirt1) and Sirtuin 2 (Sirt2) belong to the family of NAD⁺ (nicotinamide adenine dinucleotide-positive)-dependent class III histone deacetylases and are involved in regulating lifespan. As cancer is a disease of ageing, targeting Sirtuins is emerging as a promising antitumour strategy. Here we present Salermide (*N*-{3-[(2-hydroxynaphthalen-1-ylmethylene)-amino]-phenyl}-2-phenyl-propionamide), a reverse amide with a strong *in vitro* inhibitory effect on Sirt1 and Sirt2. Salermide was well tolerated by mice at concentrations up to 100 μM and prompted tumour-specific cell death in a wide range of human cancer cell lines. The antitumour activity of Salermide was primarily because of a massive induction of apoptosis. This was independent of global tubulin and K16H4 acetylation, which ruled out a putative Sirt2-mediated apoptotic pathway and suggested an *in vivo* mechanism of action through Sirt1. Consistently with this, RNA interference-mediated knockdown of Sirt1, but not Sirt2, induced apoptosis in cancer cells. Although p53 has been reported to be a target of Sirt1, genetic p53 knockdowns showed that the Sirt1-dependent proapoptotic effect of Salermide is p53-independent. We were finally able to ascribe the apoptotic effect of Salermide to the reactivation of proapoptotic genes epigenetically repressed exclusively in cancer cells by Sirt1. Taken together, our results underline Salermide's promise as an anticancer drug and provide evidence for the molecular mechanism through which Sirt1 is involved in human tumorigenesis.

Oncogene (2009) 28, 781–791; doi:10.1038/onc.2008.436; published online 8 December 2008

Keywords: HDACs inhibitors; Sirtuins; cancer; apoptosis

Introduction

Histone deacetylases (HDACs) comprise a superfamily of proteins involved in a wide range of cellular functions, which include regulation of transcription (Minucci and Pelicci, 2006; Xu *et al.*, 2007). Histone deacetylases are divided into four classes (I–IV) and regulate the expression and activity of numerous proteins involved in cancer (Glozak and Seto, 2007), which makes them promising anticancer targets (Minucci and Pelicci, 2006; Marks, 2007; Marks and Breslow, 2007). Indeed, several class I, II and IV HDAC inhibitors are currently being tested in phase I, II (reviewed in Marks, 2007; Marks and Breslow, 2007 and Xu *et al.*, 2007) and III (<http://clinicaltrials.gov>) clinical trials and one inhibitor, suberoylanilide hydroxamic acid (SAHA), is already on market.

Class III HDACs were discovered more recently and their activity is not affected by class I, II and IV inhibitors (Xu *et al.*, 2007). They include two members of the Sirtuin family of NAD⁺-dependent deacetylases: Sirtuin 1 (Sirt1) and Sirtuin 2 (Sirt2). They are involved in multiple cellular events, including transcriptional silencing, chromatin remodelling, mitosis and lifespan duration (Longo and Kennedy, 2006). In mammals, substrates for Sirt1 include histones (mainly lysine 16 of histone H4) (Vaquero *et al.*, 2004; Pruitt *et al.*, 2006), but also key transcription factors, such as p53 and forkhead transcription factors (reviewed in Fraga *et al.*, 2007). Sirt2 was initially reported to be a

Correspondence: Dr MF Fraga, Cancer Epigenetics Laboratory, Spanish National Cancer Centre (CNIO), Melchor Fernández Almagro, 3, Madrid E-28029, Spain.

E-mails: mffraga@cnio.es and mffraga@cnb.csic.es or Dr M Esteller, Cancer Epigenetics and Biology Program (PEBC), Catalan Institute of Oncology (ICO), Barcelona, Spain.

E-mail: mesteller@cnio.es

Received 8 May 2008; revised 17 October 2008; accepted 3 November 2008; published online 8 December 2008

cytoplasmic tubulin deacetylase (North *et al.*, 2003) and has subsequently been shown to deacetylate K16H4 at a global level (Vaquero *et al.*, 2006). Sirt1 and Sirt2 functions are frequently altered in cancer cells (reviewed in Fraga *et al.*, 2007) and for this reason they are starting to be considered as targets for antitumorigenic therapy.

The first-known Sirtuin inhibitors can be classified into two groups: the substances that inhibit NAD⁺ dependent reactions in general, such as nicotinamide (Bitterman *et al.*, 2002; Avalos *et al.*, 2005), and Sirtuin-specific inhibitors, such as splitomicin (Bedalov *et al.*, 2001), sirtinol (Ota *et al.*, 2006), cambinol (Heltweg *et al.*, 2006), dihydrocoumarin (Olaharski *et al.*, 2005) and some indoles (Napper *et al.*, 2005). Their common feature is that they have antitumour properties. However, their effects are generally dependent on the tumour type and stress conditions, the molecular mechanisms of action are varied or are still unclear, and the effect on non-tumorigenic samples has not been studied thoroughly. Here we describe the synthesis and mechanism of action of Salermide (*N*-{3-[(2-hydroxy-naphthalen-1-ylmethylene)-amino]-phenyl}-2-phenyl-propionamide), a new molecule with a potent inhibitory effect on Sirt1 and Sirt2.

Results and discussion

Design and synthesis of Salermide

One of the Sirtuin inhibitors with the strongest antitumour activity is sirtinol (Grozingler *et al.*, 2001). However, the inhibitory activity of sirtinol on Sirt1, one of the most important Sirtuin targets in cancer, and that has been shown to be unregulated in many tumour types, is much lower than that of Sirt2 (Mai *et al.*, 2005) and weak in general terms. Thus, we undertook molecular modelling to modify sirtinol's structure rationally in order to generate a stronger Sirtuin inhibitor. Sirtinol has a 2-hydroxy-1-naphthaldehyde moiety linked to a 2-amino-*N*-(1-phenylethyl) benzamide portion through an aldimine linkage. In considering the 3D structure of the Sirtuin C-pocket (Protein Data Bank Entry 1J8F), we wondered whether by changing the amide moiety borne by sirtinol into a reverse amide and finally shifting the amide side chain from the 2' to the 3' position of the phenyl ring a molecule that more strongly inhibited Sirtuins would be produced as it would be better adapted to their enzymatic active centre (Figure 1a). To test this hypothesis, we modelled the complexes of sirtinol and its reverse amide regioisomer, which we call Salermide, with human Sirt2-HDAC by docking these two ligands onto the C-pocket of Sirt2 structure (Protein Data Bank Entry 1J8F) and then minimizing the energy of the complex. According to these modelling studies, the binding mode and residues involved are quite well conserved for these two small molecules (Figure 1b), the hydrophobic π - π contacts being maintained with the same residues: F119 and H187. However, the change of

the amide moiety borne by sirtinol into a reverse amide in Salermide places the key chemical features for this functionality at different spatial orientations. Thus, a polar interaction is missed by sirtinol: the hydrogen bridge between the oxygen of the amide and the Q167 side chain. However, this is retained by Salermide, suggesting that this drug could constitute a better inhibitor than sirtinol, as earlier experiments showed that Q167 is crucial for HDAC-Sirt2 activity (Finnin *et al.*, 2001). In addition, it is noted that these key binding residues also match one of those reported for EX527 and Sirt1, Q345 (Q167 correspondingly on Sirt2) (Huhtiniemi *et al.*, 2006). Quantification of their corresponding interactions with Sirt2, docking fitness function and a more detailed analysis after energy minimization suggests that Salermide—the stronger inhibitor—may have a higher binding affinity than sirtinol. We then synthesized the derivative Salermide by condensation between the commercially available 2-hydroxy-1-naphthaldehyde and the *N*-(3-amino-phenyl)-2-phenyl-propionamide, which is prepared by reacting 2-phenylpropionic acid activated with BOP-reagent with 1,3-phenylenediamine under basic conditions (Figure 1c).

Salermide inhibits Sirt1 and Sirt2 in vitro

To evaluate the *in vitro* inhibitory potential of Salermide on Sirt1 and Sirt2, we incubated recombinant His-tagged human Sirt1 and Sirt2 proteins (Figure 2a) with increasing amounts of Salermide and measured HDAC activity with a fluorescent assay (Figure 2b and Supplementary Figure 1 online). We used sirtinol as the reference drug. When tested against Sirt1, Salermide showed a dose-dependent inhibition that rose to 80% at 90 μ M (Supplementary Figure 1 online). The same concentration of sirtinol resulted in a reduction of Sirt1 activity of <5% (Figure 2b). Compared with Sirt1, Salermide was even more efficient at inhibiting Sirt2, with 80% inhibition at 25 μ M (Figure 2b). At this concentration, sirtinol did not inhibit Sirt2. Thus, as predicted by the 3D modelling, Salermide is a stronger Sirtuin inhibitor than sirtinol and, more importantly, it is able to inhibit most of the Sirt1 activity (80%) at a concentration of 100 μ M, whereas the same concentration of sirtinol has a much smaller effect.

Salermide induces apoptosis in cancer but not in normal cells

Having corroborated the strong *in vitro*-inhibitory effect of Salermide on Sirt1 and Sirt2, we evaluated its potential antitumour effect. To this end, we incubated six cancer cell lines derived from leukaemia (MOLT4, KG1A, K562), lymphoma (Raji), colon (SW480) and breast (MDA-MB-231) primary malignancies in the presence of increasing concentrations of Salermide, and quantified cell proliferation with the 3-(4,5-dimethylthiazol-2-yl)-2,5-diphenyltetrazolium bromide assay. We used MRC5 *in vitro*-cultured fibroblasts as non-tumorigenic control samples. Treatment with 100 μ M Salermide for 24 h caused a decrease in the

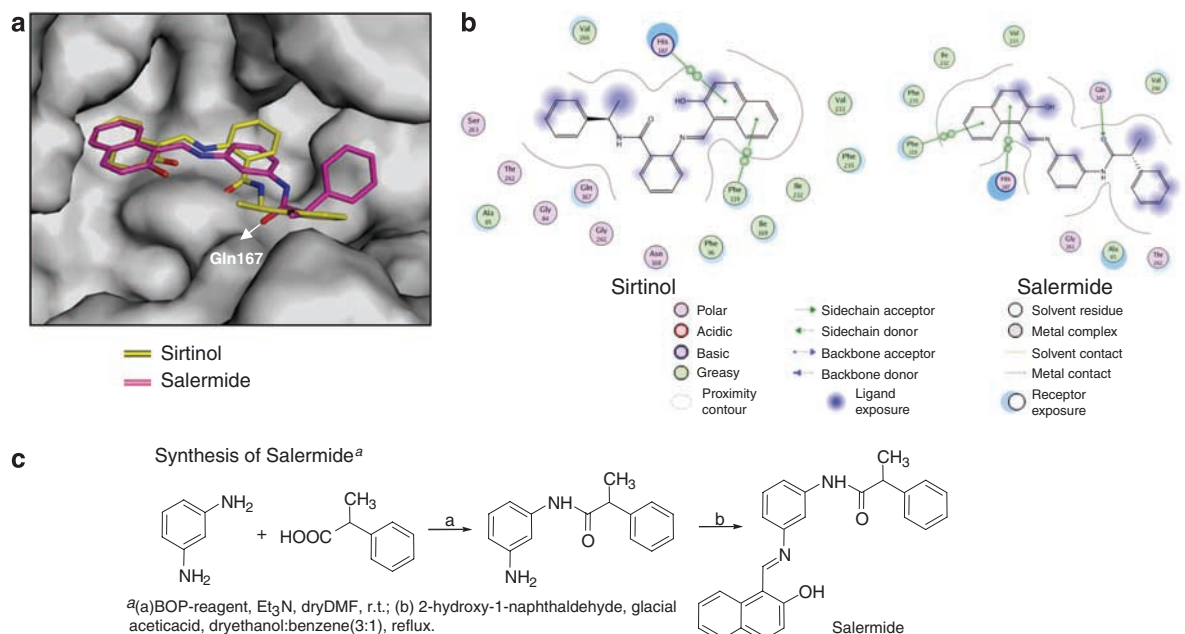


Figure 1 Design and synthesis of Salermide. (a) Structures of the complexes sirtinol/Salermide with human Sirt2 histone deacetylase modelled by docking these two ligands onto the C-pocket of Sirt2 structure after minimization. The white arrow shows the polar interaction between the carbonyl group of the amide of Salermide and Gln167 of Sirt1, which is absent in the case of sirtinol. (b) Schemes of proposed interactions obtained from docking and modelling studies, after minimization, for sirtinol and Salermide. (c) Salermide (*N*-{3-[(2-hydroxy-naphthalen-1-ylmethylene)-amino]-phenyl}-2-phenyl-propionamide) was synthesized by condensation between the commercially available 2-hydroxy-1-naphthaldehyde and the *N*-(3-amino-phenyl)-2-phenyl-propionamide, its time prepared through reaction of 2-phenylpropionic acid activated with BOP-reagent with 1,3-phenylenediamine under basic conditions. r.t., room temperature.

number of cells of all the cancer samples but not in the number of non-tumorigenic MRC5 cells (Figure 2c and Supplementary Table 1 online). The reduction in the number of cells was dependent on the cell type, as shown by the half-maximal inhibitory concentration (IC50 index) (Figure 2d). The strongest effects were observed in the leukaemia cell lines MOLT4 (Figure 2e) and KG1A in which, after 72 h of incubation with 100 μ M Salermide, only 10–20% of the initial cultured cells were viable (Supplementary Table 1 online). For the same incubation time and concentration, around 50% of the colon cancer (SW480) and lymphoma (Raji) cells were viable (Supplementary Table 1 online). In the breast cancer cell line MDA-MB-231, however, the effect was more discrete, with 90% of the cells viable after 72 h of incubation with 100 μ M Salermide (Supplementary Table 1 online). Strikingly, after 24 h of incubation with 100 μ M Salermide—the same conditions as used with the tumorigenic samples—most (95%) of the non-tumorigenic MRC5 *in vitro*-cultured fibroblasts remained viable (Figure 2c and Supplementary Table 1 online). The significantly lower IC50 of Salermide in cell lines derived from leukaemia and lymphoma primary tumours (Figure 2d) suggests a very strong inhibition effect of Salermide on blood malignancies. Compared with sirtinol, Salermide always exhibited greater inhibitory activity, but this was most evident in leukaemia and lymphoma cells (Supplementary Table 1 online). After 72 h of incubation with 100 μ M Salermide, around 10% of KG1A cells and 50% of Raji and K562 cells were viable, while after incubation with sirtinol under the

same conditions around 60% of KG1A and most (95%) of the Raji and K562 cells were viable. Consistent with this, IC50s for lymphoma and leukaemia cells were much lower in the case of Salermide than for sirtinol (Figure 2d).

To determine the cellular pathways by which Salermide exerts its antitumour-specific effects, we studied its action on apoptosis and cell-cycle progression in the same cell lines as used for the proliferation experiments. The classical class I, II and IV HDAC inhibitors induce tumour-cell death, with all of the biochemical and morphological characteristics of apoptosis (Mariadason, 2008). The earlier described class III HDAC inhibitors can also induce apoptosis, although the effect depends on the tumour type and stress conditions (Heltweg *et al.*, 2006). Other Sirtuin inhibitors have been shown to induce senescent-like growth arrest in breast and lung cancer cell lines (Ota *et al.*, 2006). Salermide induced strong apoptosis without any evident effect on the cell cycle (data not shown) in all the cancer cell lines analysed except in non-tumorigenic MRC5 cells (Figure 3a). The induction of apoptosis was cell-type-specific and dose-dependent (Figures 3a and b, respectively). Consistent with the results of the proliferation experiments, the strongest effects were observed in the MOLT4-leukaemia cell line, in that 75% of the cells underwent apoptosis after 24 h of incubation with 100 μ M Salermide (Figure 3a). To investigate further whether the induction of apoptosis by Salermide is mediated by classical apoptotic pathways, we analysed the cytosolic levels of cytochrome *c* and activated

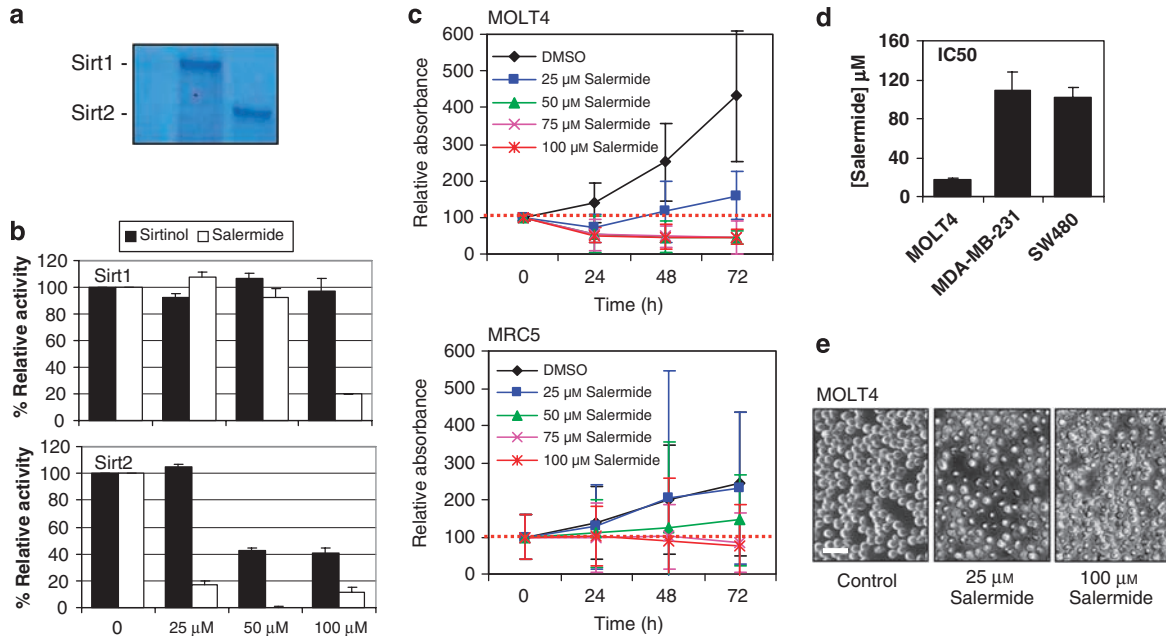


Figure 2 Sirt1 and Sirt2 *in vitro* inhibition and cancer-specific cell death induction by Salermide. (a) Coomassie brilliant dye staining of recombinant His-tagged human Sirt1 and Sirt2 proteins. (b) *In vitro* inhibition assays of Sirt1 and Sirt2 by sirtinol (black bars) and Salermide (white bars). Recombinant His-tagged human Sirt1 and Sirt2 were purified and assayed for deacetylase activity using the HDAC fluorescent activity assay. Results are expressed as the relative activity versus the activity of the enzyme not treated with sirtinol or Salermide. (c) 3-(4,5-dimethylthiazol-2-yl)-2,5-diphenyltetrazolium bromide (MTT) assay. MOLT4 and MRC5 cells were incubated with different concentrations of Salermide and DMSO (negative control) and the relative amount of viable cells were estimated by measuring the absorbance of the cell suspension after incubation with yellow MTT (a tetrazole). (d) IC₅₀ of Salermide in MOLT4, MDA-MB-231 and SW480 cancer cell lines after 24-h treatment. Cells were incubated with or without the Salermide using 0, 25, 50, 75 or 100 μM doses; an MTT assay was then carried out and a graph of viability versus drug concentration was used to calculate IC₅₀ values for each cell line. (e) Representative phase-contrast microscopy images of MOLT4 cells before and after treatment with 25 and 100 μM Salermide.

caspase 3, two well-known mediators of apoptotic pathways. We found that incubation with 100 μM Salermide alone resulted in an increase of cytosolic-activated caspase 3 and a decrease of mitochondrial-cytochrome *c* soon after 2 h of treatment, and that the levels remained elevated until 24 h of incubation, when most of the cells died. These data are evidence that Salermide alone can induce apoptosis that, in principle, could be mediated through both extrinsic and intrinsic pathways. Thus, Salermide had several antitumorigenic advantages over the earlier described class III HDAC inhibitors: firstly, it mimics the universal proapoptotic effect on cancer samples exhibited by the classical class I, II and IV HDAC inhibitors, and secondly, its proapoptotic effect is cancer-specific, as the non-tumorigenic fibroblasts MRC5 were refractory to apoptosis induction in response to this drug.

Finally, we were prompted to assess possible adverse effects of Salermide *in vivo*. To do this, we used intraperitoneal injection to administer doses of 100 μl of 100 μM of Salermide to a group of 10 nude mice over 34 days. Salermide feeding did not produce any adverse health effects in mice as monitored by diet consumption, body-weight gain, and postural and behavioural changes throughout the study. In accordance with these standards, we observed that intraperitoneal feeding of Salermide had no apparent toxicity in nude mice.

Induction of apoptosis in cancer cells by Salermide is not primarily mediated by Sirt2

Once it had been determined that Salermide antitumour activity is primarily because of the promotion of apoptosis, we decided to study the molecular mechanisms involved in this process. As Salermide has a stronger inhibitory effect on Sirt2 than on Sirt1, we first studied the role of Sirt2 in Salermide-mediated apoptosis. We knocked down Sirt2 in the MOLT4 cell line (Figure 4a, left panel) and then treated these cells with 25 μM Salermide (which corresponds to the IC₅₀ in MOLT4 cells) (Figure 4a, right panel). We observed that knocking down Sirt2 in MOLT4 cells alone did not affect apoptosis, and that the induction of apoptosis by Salermide was very similar in cells deficient in Sirt2 and in control cells (Figure 4a, right panel). Thus, in spite of Salermide being more effective *in vitro* against Sirt2 than against Sirt1, our results suggest that its *in vivo* biological role is independent of Sirt2. To demonstrate further this independence, we studied the effect of Salermide on the acetylation of two primary targets of Sirt2, namely tubulin (North *et al.*, 2003) and lysine 16 of histone H4 (K16H4) (Vaquero *et al.*, 2006), as well as its relationship with the induction of apoptosis. We incubated the aforementioned cancer cell lines with 25 and 100 μM Salermide for 24 h and then measured the levels of tubulin acetylation by immunoblot and quantified the global levels of acetylation of histone

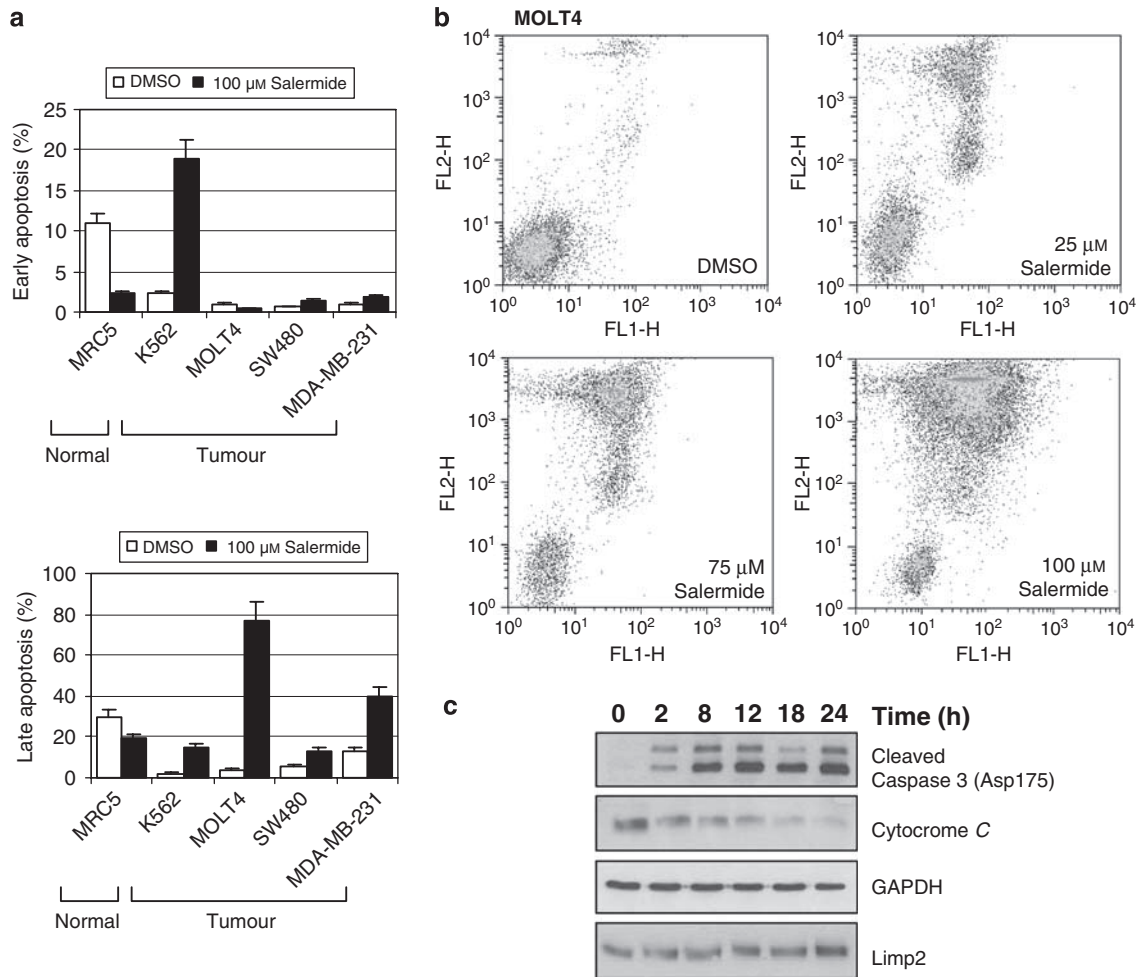


Figure 3 Salermide induces dose-dependent apoptosis in cancer cell lines but not in *in vitro*-cultured fibroblasts. (a) Relative levels of early (upper panel) and late (lower panel) apoptotic cells in cancer cell lines (K562, MOLT4, SW480 and MDA-MB-231) and *in vitro*-cultured fibroblasts (MRC5) treated with 100 μM Salermide for 24 h. Cells incubated with the vehicle (DMSO) were used as a control. The percentage of apoptotic cells was measured using the Annexin V FACS assay as described in Materials and Methods. (b) MOLT4 cells were treated with 0, 25, 75 or 100 μM of Salermide, and apoptosis was measured by flow cytometry following Annexin V (FL1-H) and PI (FL2-H) staining. Cells that are Annexin V-positive and propidium iodide (PI)-negative are in early apoptosis, as phosphatidylserine (PS) translocation has occurred, although the plasma membrane remains intact. Cells that are positive for both Annexin V and PI are either in the late stages of apoptosis or are already dead, as PS translocation has occurred and the loss of plasma membrane integrity is visible. (c) Time-course (0–24 h) western blot analysis of the proapoptotic proteins caspase 3 (cleaved isoform) and cytochrome *c* after incubation of the MOLT4 cell line with 100 μM Salermide. GAPDH and Limp2 were used as controls.

H4 by high-performance capillary electrophoresis (Fraga *et al.*, 2005) and top-down mass spectrometry (Parks *et al.*, 2007). Subsequently, we compared the levels of monoacetylated lysine 16 of histone H4 by an immunoblot and tandem mass spectrometry (Villar-Garea *et al.*, 2008). We observed that exposure to Salermide can induce slight tubulin acetylation in MOLT4 and MDA-MB-231 cells (Figure 4b). However, Salermide does not induce tubulin acetylation in the colon-cancer cell line SW480, in which the pattern of apoptosis induction is similar to that in MDA-MB-231 cells (Figure 3a). Thus, even when Salermide can affect Sirt2-dependent tubulin acetylation, its proapoptotic-mediated antitumorigenic effect does not seem to be primarily mediated by this molecular pathway. Regarding the best-characterized histone target of Sirt2, acetylation of K16H4 (Vaquero *et al.*, 2006),

high-performance capillary electrophoresis and top-down mass spectrometry experiments showed that Salermide does not significantly increase global H4 acetylation levels (Figures 4c and d) in cancer cells. Of the five cell lines analysed, we observed only a slight increase of global H4 acetylation in MDA-MB-231 (Figure 4c). Consistent with this, an immunoblot using antibodies against acetylated K16H4 showed a small increase of AcK16H4 in response to Salermide in only MDA-MB-231 cells (Figure 4e). The lack of K16H4 hyperacetylation in response to Salermide was confirmed using mass spectrometry for histone H4 from Raji cells; MALDI-TOF (matrix-assisted laser desorption/ionization time-of-flight) spectra show a decrease in mono- and diacetylation at the peptide 4–17 after Salermide treatment (Figure 4f). Tandem mass spectrometry analysis of the monoacetylated

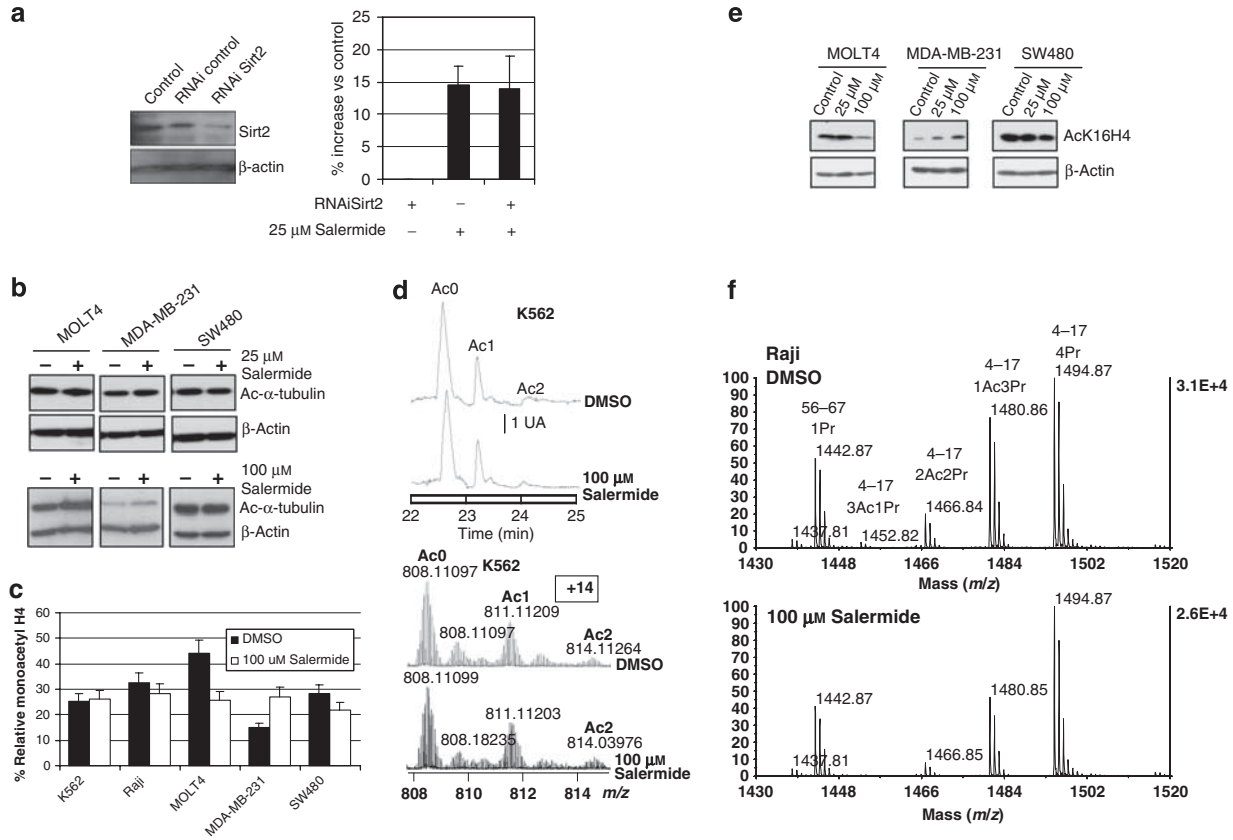


Figure 4 *In vivo* biological effects of Salermide are not primarily mediated by Sirt2. (a) The left panel shows the western blot analysis of the Sirt2 levels in MOLT4 cells (Control) and the same cells interfered with an unspecific oligo (RNAi control) or a Sirt2-specific RNAi oligo (RNAi Sirt2). An antibody against β -actin was used as a positive control. The right panel shows the relative levels of apoptotic cells, measured as described in Figure 3, in MOLT4 cells interfered or not by Sirt2-specific oligos and treated or not with 25 μ M Salermide for 24 h. The results are expressed as the relative increase of apoptotic cells in each combination of treatments compared with control cells. (b) Western blot analysis of the levels of acetylated α -tubulin in MOLT4, MDA-MB-231 and SW480 cells treated (+) or not (-) with 25 and 100 μ M Salermide for 24 h. An antibody against β -actin was used as a loading positive control. (c) Quantification of the relative levels of monoacetylated histone H4 by HPCE in the cancer cell lines K562, Raji, MOLT4, MDA-MB-231 and SW480 treated (white bars) or not (black bars) with 100 μ M Salermide for 24 h. (d) The upper panel shows representative electropherograms obtained by HPCE of the different acetylated isoforms of the histone H4 from K562 cancer cells and the same cell line treated with 100 μ M Salermide. The lower panel shows representative MS spectra of intact histone H4 from K562 cancer cells and the same cells treated with 100 μ M Salermide obtained by top-down mass spectrometry. The m/z ratio (charge +14) for each peak is shown over the MS traces. Ac0, Ac1 and Ac3 stand for non-, mono- and diacetylated histone H4 isoforms, respectively. (e) Western blot analysis of the levels of acetylated lysine 16 histone H4 (AcK16H4) in MOLT4, MDA-MB-231 and SW480 cells treated or not with 25 and 100 μ M Salermide for 24 h. An antibody against β -actin was used as a loading positive control. (f) MALDI time-of-flight analysis of histone H4 obtained from Raji cancer cells and the same cell line treated with 100 μ M Salermide for 24 h. Histone H4 was purified through SDS-PAGE, propionylated and digested as described in Materials and Methods. A zoom of the spectra on the region containing the signals for the peptide 4-17 of H4 is shown. Note that the peptide with the highest m/z carries four propionyl groups and corresponds to the unmodified form *in vivo*.

peptide indicates that in both treated and untreated samples most of the monoacetylation occurs at K16H4 (data not shown), which indicates that Salermide treatment does not increase K16H4 acetylation in Raji cells. Thus, taken together, our results suggest that the proapoptotic antitumorigenic effect of Salermide does not seem to be primarily mediated either directly or indirectly by Sirt2. It is important to note that these results do not necessarily imply that Salermide cannot inhibit Sirt2 *in vivo*. However, the effect that Salermide has on other targets is probably faster and, as the cells enter apoptosis, there is insufficient time to observe the biological effects mediated by Sirt2.

Induction of apoptosis in cancer cells by Salermide is primarily mediated by Sirt1

We next focused our attention on Sirt1. Its participation in the biological response of cancer cells to Salermide is indicated by the fact that RNA interference (RNAi)-mediated knockdown of Sirt1 results in increased apoptosis in various cancer cell lines (Chen *et al.*, 2005; Ford *et al.*, 2005; Pruitt *et al.*, 2006; Wang *et al.*, 2006; Stunkel *et al.*, 2007; Sun *et al.*, 2007). To show further Sirt1's specific role in inducing apoptosis in cancer cells in response to Salermide, we used RNAi methodology to knock down Sirt1 activity in the MOLT4 cell line (Figure 5a, left panel) and then treated these cells with 25 μ M Salermide (Figure 5a, right panel). We observed

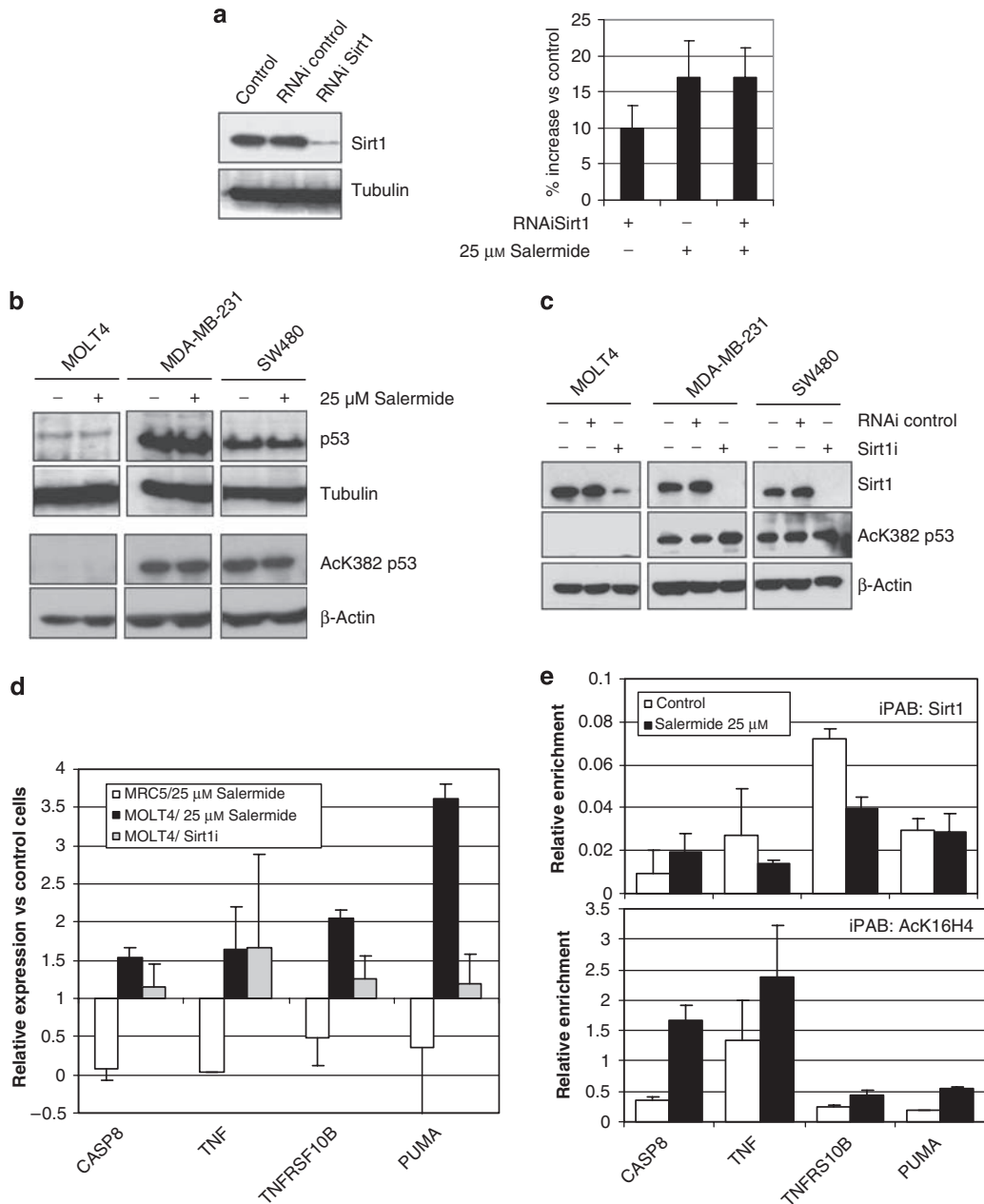


Figure 5 *In vivo* biological effects of Salermide are primarily mediated by Sirt1. (a) The left panel shows the western blot analysis of the Sirt1 levels in MOLT4 cells treated with an RNAi control and the same cells treated with RNAi against Sirt1. An antibody against α -tubulin was used as a loading positive control. The right panel shows the relative levels of apoptotic cells, measured as described in Figure 3, in MOLT4 cells interfered or not by Sirt1-specific oligos and treated or not with 25 μ M Salermide for 24 h. The results are expressed as the relative increase of apoptotic cells in each combination of treatments compared with control cells. (b) Western blot analysis of the levels of p53 and p53 acetylated at lysine 382 in MOLT4, MDA-MB-231 and SW480 cells treated (+) or not (-) with 25 μ M Salermide for 24 h. Antibodies against α -tubulin and β -actin were used as loading controls for p53 and AcK382 p53, respectively. (c) Western blot analysis of the levels of Sirt1 and p53 acetylated at lysine 382 in MOLT4, MDA-MB-231 and SW480 cells interfered with an unspecific oligo (RNAi control) or a Sirt1-specific RNAi oligo (Sirt1i). Antibody against β -actin was used as the loading control. (d) Relative expression levels of selected proapoptotic genes reactivated after treatment with 25 μ M Salermide in MOLT4 cancer cells (black bars). White bars show the relative expression levels of the same genes in MRC5 fibroblasts treated with the same concentration of Salermide; grey bars indicate the expression after Sirt1 interference in MOLT4 cells. (e) Determination of promoter occupancy at the CASP8, TNF, TNFRSF10B and PUMA genes by quantitative ChIP in the MOLT4 cell line treated (black bars) or not (white bars) with 25 μ M Salermide. The antibodies (iP AB) were against Sirt1 and histone H4 acetylated at lysine 16 (AcK16H4). Fold enrichment refers to the copy number of a gene of interest in the bound fraction after chromatin immunoprecipitation with the appropriate antibody divided by the copy number of that gene in the bound fraction after ChIP with the H3 antibody (positive control).

that knocking down Sirt1 activity in MOLT4 cells alone induced 10% apoptosis (Figure 5a, right panel). Treatment with 25 μ M Salermide induced around 16% apoptosis, a percentage that was almost identical in Sirt1-deficient cells (Figure 5a, right panel). The slightly higher degree of apoptosis obtained with Salermide than with RNAi Sirt1 can be explained by the fact that, on average, only 70% of the MOLT4 cells become transfected with the RNAi Sirt1 construct (data not shown). Thus, as treatment with Salermide and RNAi Sirt1 induce a similar degree of apoptosis, these results support the idea that Salermide's mechanism of action *in vivo* is specifically mediated by Sirt1. In addition, as combined treatment with Salermide and RNAi Sirt1 does not result in greater apoptotic induction than treatment with Salermide alone, it seems likely that the induction of apoptosis in MOLT4 cells with 25 μ M Salermide is primarily mediated by Sirt1 alone.

To study the involvement of Sirt1 in the apoptotic response of cancer cells to Salermide in greater depth, we examined the acetylation status of several Sirt1 targets in cells before and after treatment with 25 μ M Salermide. One of the primary molecular targets of Sirt1 is p53 (Vaziri *et al.*, 2001). Sirt1 is able to deacetylate and inhibit p53 increasing survival in response to stress (Luo *et al.*, 2001). Thus, we hypothesized that inhibiting Sirt1 could activate p53 and induce apoptosis. To test this, we used immunoblot to determine the acetylation status of p53 in response to Salermide in the MOLT4, MDA-MB-231 and SW480 cell lines. Intriguingly, we observed that, as proposed earlier, MOLT4 presents very reduced levels of the p53 tumour suppressor protein (Figure 5b; Rodrigues *et al.*, 1990) which, given that Salermide induces apoptosis in MOLT4, rules out the possibility of a principal role for p53 in the process. We did not observe a significant increase in p53 acetylation in response to 25 μ M Salermide in the MDA-MB-231 and SW480 cell lines (Figure 5b). To examine the role of Sirt1 in p53 acetylation in greater detail, we used RNAi methodology to knock down Sirt1 activity in the MOLT4, MDA-MB-231 and SW480 cell lines (Figure 5c). We found that interfering Sirt1 induces only a moderate increase of p53 acetylation in the MDA-MB-231 cell line. Consistent with this, treatment with 100 μ M Salermide (the concentration necessary to achieve the IC₅₀ in MDA-MB-231 cells) induced a similar increase of p53 acetylation in this breast cancer cell line (data not shown). The effect of Sirt1 on p53 acetylation in cancer is variable. Various other researchers have reported that Sirt1 inhibition can induce (Heltweg *et al.*, 2006; Lain *et al.*, 2008) or not induce (Ota *et al.*, 2006) p53 acetylation in cancer cell lines. As we found induction of p53 acetylation in response to Salermide-mediated Sirt1 inhibition only in the MDA-MB-231 cell line, our results suggest that the role of Sirt1 in p53 acetylation depends on the cell type.

We found that Salermide can induce apoptosis without increasing p53 acetylation (SW480 cells) and that it can even do it in cells deficient in p53 (MOLT4). This is consistent with earlier work showing that Sirt1 inhibition in MCF-7 breast cancer cell line (Ota *et al.*, 2006) does

not induce p53 acetylation, and that RNAi-mediated knockout of Sirt1 p53-deficient HCT116 colon cancer cells induces apoptosis (Ford *et al.*, 2005). Overall, these observations imply that p53 may be dispensable for the induction of Sirt1-dependent apoptosis in cancer cells. This is in close agreement with the finding in Sirt1/p53 double-knockout mice that Sirt1 does not affect p53-dependent apoptosis (Kamel *et al.*, 2006).

Salermide induces the reactivation of proapoptotic genes that are aberrantly repressed in cancer cells by Sirt1-mediated K16H4 deacetylation

We next turned our attention to the locus-specific acetylation of lysine 16 of histone H4, the main histone target of Sirt1 (Vaquero *et al.*, 2004). It has recently been proposed that some of the protumorigenic effects of Sirt1 are mediated by the aberrant recruitment of Sirt1 to the promoter region of tumour suppressor genes (TSGs) and subsequent aberrant epigenetic repression (Pruitt *et al.*, 2006). As Salermide induces massive apoptosis in less than 24 h after treatment, we formulated the hypothesis that Sirt1 was aberrantly recruited to proapoptotic genes in cancer but not in normal cells, and, as a consequence of that, these genes were aberrantly repressed in cancer cells. The treatment with Salermide would thus induce apoptosis through the inhibition of Sirt1 and consequent hyperacetylation and reactivation of these genes. To test this hypothesis, we first used the TaqMan Low Density Array Human Apoptosis Panel (Applied Biosystems) to analyse the expression status of 93 genes involved in apoptosis in the MOLT4 cancer cell line and the MRC5 fibroblasts before and after incubation with 25 μ M Salermide. Intriguingly, we found that 20 of the 37 (54%) proapoptotic genes in the TaqMan Low Density Array were overexpressed (>20%) after treating the MOLT4 cells with 25 μ M Salermide (Figure 5d). Of even greater note, none of these genes was overexpressed in MRC5 cells after treatment with Salermide (Figure 5d and Supplementary Table 2 online). To confirm that the reactivation of these genes is mediated by Sirt1, we used RNAi methodology to knock down Sirt1 activity in the MOLT4 cell line and then analysed the expression status of the aforementioned 93 genes. We found that 18 of the 37 (49%) proapoptotic genes in the TaqMan Low Density Array were overexpressed (>20%) after knocking down Sirt1 activity (Figure 5d and Supplementary Table 2 online). It is also noteworthy that all of these genes were also overexpressed in MOLT4 cells treated with 25 μ M Salermide (Figure 5d and Supplementary Table 2 online). As earlier argued, the greater number of proapoptotic genes reactivated with Salermide than with RNAi Sirt1 can be explained by the fact that, on average, only 70% of the MOLT4 cells become transfected with the RNAi Sirt1 construct (data not shown). Thus, the high degree of coincidence between Salermide-mediated Sirt1 inhibition and iRNA-mediated Sirt1 silencing suggests that the *in vivo* mechanism of action of Salermide is specifically mediated through Sirt1.

To discover more about the role of Sirt1 in reactivating proapoptotic genes in response to Salermide, we used chromatin immunoprecipitation technology to assess Sirt1 occupancy and the acetylation status of K16 of histone H4 in MOLT4 cells treated or not with Salermide at the promoter region of four of the reactivated genes (CASP8, TNF, TNFRSF10B and PUMA). We found that for all these four genes, their reactivation after treatment with Salermide was associated with a substantial increase in the acetylation status of the lysine 16 of histone H4 at their promoter region (Figure 5e). Interestingly, we detected Sirt1 in the promoter region of all four genes analysed (Figure 5e). These observations suggest that Sirt1 may be involved in the aberrant repression of proapoptotic genes in cancer by a mechanism that prevents the acetylation of lysine 16 of the histone H4 at their respective promoters. Most of these apoptotic genes act downstream in the death-receptor pathway, and so their aberrant epigenetic inactivation might impair the induction of apoptosis in tumour cells, which would imply that Sirt1 contributes to the promotion of cancer. The inhibition of Sirt1 with Salermide results in the reactivation of several of these genes, leading to an overall induction of apoptotic pathways as shown by the increase in cytosolic cytochrome *c* and cleaved caspase 3 after treatment with Salermide (Figure 3c). Our results not only draw attention to Salermide as a promising antitumorigenic drug, but also support the hypothesis that improper Sirt1 deacetylation of lysine16 of histone H4 at cancer-protective genes might be tumorigenic (Pruitt *et al.*, 2006). Although our results suggest that one of the molecular mechanisms by which Salermide induces apoptosis is the reactivation of proapoptotic genes aberrantly silenced by Sirt1, we cannot exclude the possibility that, apart from the reactivation of proapoptotic genes, the induction of apoptosis by Salermide can be mediated by other Sirt1 targets, such as forkhead transcriptional factors (FOXO), p300 histone acetyltransferase, the tumour protein p73 (p73), E2F transcription factor 1, the DNA repair factor Ku antigen, 70-kDa subunit (Ku70), the nuclear factor kappa-B inhibitor and the androgen receptor (reviewed in Guarente and Picard, 2005). Indeed, some targets, such as E2F transcription factor 1 and nuclear factor kappa-B inhibitor, are important players in the apoptotic pathways (reviewed in Fraga and Esteller, 2007).

Concluding remarks

Here we describe Salermide, a reverse amide at the meta position that has a strong inhibitory activity on Sirtuins. It induces massive apoptosis in cancer but not in non-transformed cultured cells, which makes it a promising candidate as a future antitumorigenic drug. We were able to establish that the apoptotic effect of Salermide is in part because of the reactivation of proapoptotic genes that are epigenetically repressed by Sirt1 exclusively in cancer cells. This provides further clarification of the molecular mechanism by which Sirt1 exerts its oncogenic effects in cancer.

Materials and methods

3D modelling

Docking studies were performed using the genetic algorithm-based program GOLD (Jones *et al.*, 1997), where GoldScore was used as scoring function to rank proposed binding solutions. The available experimental information was considered to define the docking area to be explored; thus, the docking region used was a 10-Å sphere around the oxygen O of Gln167, the Sirt2 C-pocket (Finnin *et al.*, 2001; Min *et al.*, 2001; Avalos *et al.*, 2005; Huhtiniemi *et al.*, 2006). For Salermide, all proposed solutions converged to the same binding area and mode, involving the same residues; however, different solutions emerged for sirtinol, and the five highest-ranking solutions were selected for further analyses. Thus, those complexes corresponding to the best pose for Salermide and the top five best poses for sirtinol were energy-minimized under the AMBER99 force field (Ponder and Case, 2003), using a continuum solvation model, the implicit generalized Born model (Onufriev *et al.*, 2004) and a non-bonded cutoff of 18 Å. This gave the best pose for sirtinol of the top five-ranked solutions provided by GoldScore, which was very close to Salermide; in fact, the root mean square deviation between their best poses was only 5.66 Å (for heavy atoms) (Figure 1a). The energy of interaction between Salermide and Sirt2, obtained after minimization, was -56.95 and -44.61 kcal/mol for the sirtinol-Sirt2 complex. The difference, around 12 kcal/mol, suggests that Salermide is a more potent inhibitor of Sirt2; this is in agreement with the ranking obtained through the docking fitness function. The higher estimated binding affinity of Salermide may be due, in part, to the polar interaction between the amidic carbonyl group and Q167, which sirtinol does not exhibit.

Ligands were allowed full flexibility during docking and minimization. In the case of the receptor, all backbone and side-chain torsion angles were allowed to move according to the potential used for minimization. Energy minimization was carried out with the MOE package (Chemical Computing Group, Inc. Molecular Operating Environment, MOE 2007.09 (2007), Montreal, Quebec, Canada), and the same program was used to display the schematics of the interactions between Sirt2 and the ligands (Clark *et al.*, 2006) (Figure 1b).

Synthesis of Salermide

Melting points were determined with the Buchi 530 melting point apparatus and were not corrected. Infrared (IR) spectra (KBr) were recorded on a Perkin-Elmer Spectrum One instrument. ¹H nuclear magnetic resonance spectra were recorded at 400 MHz with a Bruker AC 400 spectrometer, reporting chemical shifts in δ (ppm) units relative to the internal reference tetramethylsilane (Me₄Si). All compounds were routinely checked by thin-layer chromatography and ¹H nuclear magnetic resonance. Thin-layer chromatography was performed on aluminium-backed silica gel plates (Merck DC, Darmstadt, Alufolien Kieselgel 60 F₂₅₄) with spots visualized under ultraviolet light. All solvents were reagent grade and, when necessary, were purified and dried by standard methods. Concentrations of solutions after reactions and extractions were measured using a rotary evaporator operating at a reduced pressure of ~20 torr. Organic solutions were dried over anhydrous sodium sulphate. Analytical results were within ±0.40% of theoretical values. All chemicals were purchased from Aldrich Chimica (Milan, Italy) or Lancaster Synthesis GmbH (Milan, Italy), and were of the highest purity.

In vitro inhibition assays of Sirt1 and Sirt2

Recombinant His-tagged human Sirt1 and Sirt2 were assayed for deacetylase activity using the HDAC fluorescent activity

assay (BIOMOL, Plymouth, PA, USA) (Howitz *et al.*, 2003). Reactions were carried out at 37 °C for 60 min. Results are expressed as the mean and standard deviation of four independent experiments.

Cell lines, culture conditions and treatments

Cell lines (SW480, MDA-MB-231, MOLT4, KG1A, K562 and Raji) were obtained from the American Type Culture Collection (VA, USA). Cell viability was determined using the 3-(4,5-dimethylthiazol-2-yl)-2,5-diphenyltetrazolium bromide assay as described earlier (Ropero *et al.*, 2004). IC50 index was calculated using four Salermide concentrations (25, 50, 75 and 100 µM) for 24 h. The percentage of apoptotic cells was determined with the FACSCalibur (BD, Heidelberg, Germany) apparatus. The Annexin V FACS analysis was carried out according to the manufacturer's protocol (Annexin V-FITC, BD-Pharmingen, San Diego, CA, USA). *In vivo* tolerability of Salermide was studied in ten athymic (BALB/c, nu/nu) female nude mice (Harlan Sprague-Dawley, Indianapolis, IN, USA). Salermide (100 µM) was administered as described elsewhere (Herranz *et al.*, 2006).

Small interfering RNA interference assay

MOLT4 cells were nucleofected with validated Sirt2 RNAi (SI00301805 and SI02655471, QUIAGEN, Hilden, Germany) and Sirt1 RNAi (12938-127 duo pack, Invitrogen, Carlsbad, CA, USA) using the Cell Line Nucleofector Kit L (Amaxa Biosystems, Cologne, Germany).

Western blot analysis

Cell lysates for protein analysis were prepared and analysed by western blotting using the following antibodies: anti-acetylated tubulin (1:2000, Sigma-Aldrich, St Louis, MS, USA), anti-β-actin (1:10 000, Sigma-Aldrich), anti-acetyl-p53 lys382 (1:1000, CST, Danvers, MA, USA), anti-p53 monoclonal DO1 (1:2000, Oncogene Sciences, Cambridge, MA, USA), anti-α-tubulin (1:50 000, Sigma-Aldrich), anti-AcK16H4 (1:2000, Upstate, Billerica, MA, USA), anti-Sirt2 antibody (1:1000, Abcam, Cambridge, UK) and anti-Sirt1 antibody (1:1000, CST), anti-caspase 3 (1:1000, CST), anti-caspase 8 (1:1000, Abcam) and anti-cytochrome *c* (1:1000, CST). Cytoplasmic (40 µg) and membrane (30 µg) lysates were prepared using the Calbiochem's (San Diego, CA, USA) subcellular proteome extraction kit.

High-performance capillary electrophoresis

Histone H4 acetylation was quantified as described earlier (Fraga *et al.*, 2005). Individual histone fractions were prepared from cell nuclei and then purified by reverse-phase high-performance liquid chromatography. Acetylated histone H4 derivatives were resolved by high-performance capillary electrophoresis.

Top-down mass spectrometry

High-resolution mass measurements for exact mass determination were carried out using an APEX Qe Fourier transform mass spectrometer (Bruker Daltonics Inc., Billerica, MA,

USA) equipped with 9.4-T superconducting refrigerated cryomagnet and the external electrospray ion source (Dual source). The spectra were externally calibrated with an arginine cluster in positive ion mode in the mass range 350–1400 *m/z*. The spectra were acquired over a mass range of 200–3000 *m/z* using 1M data points. After sine apodization the spectra were processed with DataAnalysis 3.4 (Bruker Daltonik GmbH, Bremen, Germany) using SNAP2 for quantification.

MALDI-TOF and electrospray ionization-mass spectrometry/mass spectrometry

Histone H4 was prepared as described earlier (Villar-Garea *et al.*, 2008). MALDI-TOF spectra were acquired on a Voyager DE-STR station (Applied Biosystems, Weiterstadt, Germany) in positive reflector mode. Collision-induced decay spectra were recorded on a Q-STAR XL instrument (PE-Sciex, Ontario, Canada) with manually adjusted collision energies.

Quantitative RT-PCR

Relative expression levels of proapoptotic genes were analysed using the TaqMan Low Density Array Human Apoptosis Panel (Applied Biosystems, Foster City, CA, USA) and the Applied Biosystems 7900HT Fast Real-Time PCR System. Data were normalized using GAPDH and β-actin as endogenous controls.

Quantitative chromatin immunoprecipitation

The chromatin immunoprecipitation assay was carried out as described earlier (Fraga *et al.*, 2005) with anti-AcK16H4 (Active Motif, Carlsbad, CA, USA), anti-Sirt1 (CST) and anti-H3 (Abcam, Cambridge, UK) antibodies. PCR reactions were run and analysed using the Applied Biosystems 7900HT Fast Real-Time PCR System. Primers and conditions for each promoter are shown in Supplementary Table 3 online. The enrichment factor refers to the copy number of a gene of interest in the bound fraction after ChIP with the appropriate antibody divided by the copy number of that gene in the bound fraction after ChIP with the H3 antibody.

Acknowledgements

This work was primarily supported by the European Union (LSHG-CT-2006-037415). MFF is funded by the Spanish Ramon & Cajal Programme and the Health Department of the Spanish Government (PI061267). Thanks are due to PRIN2006 (AM) and AICR2007 (AM) for grants. The Cancer Epigenetics group at the CNIO is supported by the Health (FIS01-04) and Education and Science (I + D + I MCYT08-03, FU2004-02073/BMC and Consolider MEC09-05) Departments of the Spanish Government, the European Grant TRANSFOG LSHC-CT-2004-503438, EPITRON LSHC-CT-2005-518417, APO-SYS HEALTH-F4-2007-200767 and the Spanish Association Against Cancer (AECC). EL is a recipient of a fellowship from the FIS Spanish Research Program. VC is a recipient of a Fellowship from the FPU Spanish Research Program.

References

Avalos JL, Bever KM, Wolberger C. (2005). Mechanism of siruoin inhibition by nicotinamide: altering the NAD(+) cosubstrate specificity of a Sir2 enzyme. *Mol Cell* **17**: 855–868.

Bedalov A, Gatbonton T, Irvine WP, Gottschling DE, Simon JA. (2001). Identification of a small molecule inhibitor of Sir2p. *Proc Natl Acad Sci USA* **98**: 15113–15118.

- Bitterman KJ, Anderson RM, Cohen HY, Latorre-Esteves M, Sinclair DA. (2002). Inhibition of silencing and accelerated aging by nicotinamide, a putative negative regulator of yeast sir2 and human SIRT1. *J Biol Chem* **277**: 45099–45107.
- Chen WY, Wang DH, Yen RC, Luo J, Gu W, Baylin SB. (2005). Tumor suppressor HIC1 directly regulates SIRT1 to modulate p53-dependent DNA-damage responses. *Cell* **123**: 437–448.
- Clark AM, Labute P, Santavy M. (2006). 2D structure depiction. *J Chem Inf Model* **46**: 1107–1123.
- Finnin MS, Donigan JR, Pavletich NP. (2001). Structure of the histone deacetylase SIRT2. *Nat Struct Biol* **8**: 621–625.
- Ford J, Jiang M, Milner J. (2005). Cancer-specific functions of SIRT1 enable human epithelial cancer cell growth and survival. *Cancer Res* **65**: 10457–10463.
- Fraga MF, Agrelo R, Esteller M. (2007). Cross-talk between aging and cancer: the epigenetic language. *Ann N Y Acad Sci* **1100**: 60–74.
- Fraga MF, Ballestar E, Villar-Garea A, Boix-Chornet M, Espada J, Schotta G et al. (2005). Loss of acetylation at Lys16 and trimethylation at Lys20 of histone H4 is a common hallmark of human cancer. *Nat Genet* **37**: 391–400.
- Fraga MF, Esteller M. (2007). Epigenetics and aging: the targets and the marks. *Trends Genet* **23**: 413–418.
- Glozak MA, Seto E. (2007). Histone deacetylases and cancer. *Oncogene* **26**: 5420–5432.
- Grozinger CM, Chao ED, Blackwell HE, Moazed D, Schreiber SL. (2001). Identification of a class of small molecule inhibitors of the sirtuin family of NAD-dependent deacetylases by phenotypic screening. *J Biol Chem* **276**: 38837–38843.
- Guarente L, Picard F. (2005). Calorie restriction—the SIR2 connection. *Cell* **120**: 473–482.
- Heltweg B, Gatbonton T, Schuler AD, Posakony J, Li H, Goehle S et al. (2006). Antitumor activity of a small-molecule inhibitor of human silent information regulator 2 enzymes. *Cancer Res* **66**: 4368–4377.
- Herranz M, Martin-Caballero J, Fraga MF, Ruiz-Cabello J, Flores JM, Desco M et al. (2006). The novel DNA methylation inhibitor zebularine is effective against the development of murine T-cell lymphoma. *Blood* **107**: 1174–1177.
- Howitz KT, Bitterman KJ, Cohen HY, Lamming DW, Lavu S, Wood JG et al. (2003). Small molecule activators of Sirtuins extend *Saccharomyces cerevisiae* lifespan. *Nature* **425**: 191–196.
- Huhtiniemi T, Wittekindt C, Laitinen T, Leppanen J, Salminen A, Poso A et al. (2006). Comparative and pharmacophore model for deacetylase SIRT1. *J Comput Aided Mol Des* **20**: 589–599.
- Jones G, Willett P, Glen RC, Leach AR, Taylor R. (1997). Development and validation of a genetic algorithm for flexible docking. *J Mol Biol* **267**: 727–748.
- Kamel C, Abrol M, Jardine K, He X, McBurney MW. (2006). SirT1 fails to affect p53-mediated biological functions. *Aging Cell* **5**: 81–88.
- Lain S, Hollick JJ, Campbell J, Staples OD, Higgins M, Aoubala M et al. (2008). Discovery, *in vivo* activity, and mechanism of action of a small-molecule p53 activator. *Cancer Cell* **13**: 454–463.
- Longo VD, Kennedy BK. (2006). Sirtuins in aging and age-related disease. *Cell* **126**: 257–268.
- Luo J, Nikolaev AY, Imai S, Chen D, Su F, Shiloh A et al. (2001). Negative control of p53 by Sir2alpha promotes cell survival under stress. *Cell* **107**: 137–148.
- Mai A, Massa S, Lavu S, Pezzi R, Simeoni S, Ragno R et al. (2005). Design, synthesis, and biological evaluation of sirtinol analogues as class III histone/protein deacetylase (Sirtuin) inhibitors. *J Med Chem* **48**: 7789–7795.
- Mariadason JM. (2008). HDACs and HDAC inhibitors in colon cancer. *Epigenetics* **3**: 28–37.
- Marks PA. (2007). Discovery and development of SAHA as an anticancer agent. *Oncogene* **26**: 1351–1356.
- Marks PA, Breslow R. (2007). Dimethyl sulfoxide to vorinostat: development of this histone deacetylase inhibitor as an anticancer drug. *Nat Biotechnol* **25**: 84–90.
- Min J, Landry J, Sternglanz R, Xu RM. (2001). Crystal structure of a SIR2 homolog–NAD complex. *Cell* **105**: 269–279.
- Minucci S, Pelicci PG. (2006). Histone deacetylase inhibitors and the promise of epigenetic (and more) treatments for cancer. *Nat Rev Cancer* **6**: 38–51.
- Napper AD, Hixon J, McDonagh T, Keavey K, Pons JF, Barker J et al. (2005). Discovery of indoles as potent and selective inhibitors of the deacetylase SIRT1. *J Med Chem* **48**: 8045–8054.
- North BJ, Marshall BL, Borra MT, Denu JM, Verdin E. (2003). The human Sir2 ortholog, SIRT2, is an NAD⁺-dependent tubulin deacetylase. *Mol Cell* **11**: 437–444.
- Olaharski AJ, Rine J, Marshall BL, Babiarczyk J, Zhang L, Verdin E et al. (2005). The flavoring agent dihydrocoumarin reverses epigenetic silencing and inhibits sirtuin deacetylases. *PLoS Genet* **1**: e77.
- Onufriev A, Bashford D, Case DA. (2004). Exploring protein native states and large-scale conformational changes with a modified generalized born model. *Proteins* **55**: 383–394.
- Ota H, Tokunaga E, Chang K, Hikasa M, Iijima K, Eto M et al. (2006). Sirt1 inhibitor, Sirtinol, induces senescence-like growth arrest with attenuated Ras-MAPK signaling in human cancer cells. *Oncogene* **25**: 176–185.
- Parks BA, Jiang L, Thomas PM, Wenger CD, Roth MJ, Boyne II MT et al. (2007). Top-down proteomics on a chromatographic time scale using linear ion trap Fourier transform hybrid mass spectrometers. *Anal Chem* **79**: 7984–7991.
- Ponder JW, Case DA. (2003). Force fields for protein simulations. *Adv Protein Chem* **66**: 27–85.
- Pruitt K, Zinn RL, Ohm JE, McGarvey KM, Kang SH, Watkins DN et al. (2006). Inhibition of SIRT1 reactivates silenced cancer genes without loss of promoter DNA hypermethylation. *PLoS Genet* **2**: e40.
- Rodriguez NR, Rowan A, Smith ME, Kerr IB, Bodmer WF, Gannon JV et al. (1990). p53 mutations in colorectal cancer. *Proc Natl Acad Sci USA* **87**: 7555–7559.
- Ropero S, Menendez JA, Vazquez-Martin A, Montero S, Cortes-Funes H, Colomer R. (2004). Trastuzumab plus tamoxifen: anti-proliferative and molecular interactions in breast carcinoma. *Breast Cancer Res Treat* **86**: 125–137.
- Stunkel W, Peh BK, Tan YC, Nayagam VM, Wang X, Salto-Tellez M et al. (2007). Function of the SIRT1 protein deacetylase in cancer. *Biotechnol J* **2**: 1360–1368.
- Sun Y, Sun D, Li F, Tian L, Li C, Li L et al. (2007). Downregulation of Sirt1 by antisense oligonucleotides induces apoptosis and enhances radiation sensitization in A549 lung cancer cells. *Lung Cancer* **58**: 21–29.
- Vaquero A, Scher M, Lee D, Erdjument-Bromage H, Tempst P, Reinberg D. (2004). Human SirT1 interacts with histone H1 and promotes formation of facultative heterochromatin. *Mol Cell* **16**: 93–105.
- Vaquero A, Scher MB, Lee DH, Sutton A, Cheng HL, Alt FW et al. (2006). SirT2 is a histone deacetylase with preference for histone H4 Lys 16 during mitosis. *Genes Dev* **20**: 1256–1261.
- Vaziri H, Dessain SK, Ng Eaton E, Imai SI, Frye RA, Pandita TK et al. (2001). hSIR2(SIRT1) functions as an NAD-dependent p53 deacetylase. *Cell* **107**: 149–159.
- Villar-Garea A, Israel L, Imhof A. (2008). Analysis of histone modifications by mass spectrometry. *Curr Protoc Prot Sci* (Chapter 14, Unit 14 10).
- Wang C, Chen L, Hou X, Li Z, Kabra N, Ma Y et al. (2006). Interactions between E2F1 and SirT1 regulate apoptotic response to DNA damage. *Nat Cell Biol* **8**: 1025–1031.
- Xu WS, Parmigiani RB, Marks PA. (2007). Histone deacetylase inhibitors: molecular mechanisms of action. *Oncogene* **26**: 5541–5552.

Supplementary Information accompanies the paper on the Oncogene website (<http://www.nature.com/onc>)